Reactions of Gadolinium Atoms and Dimers with CO: Formation of Gadolinium Carbonyls and Photoconversion to CO Activated Molecules

Xi Jin,[†] Ling Jiang,[‡] Qiang Xu,*[,‡] and Mingfei Zhou*[,†]

Department of Chemistry & Laser Chemistry Institute, Shanghai Key Laboratory of Molecular Catalysts and Innovative Materials, Fudan University, Shanghai 200433, P. R. China, and National Institute of Advanced Industrial Science and Technology (AIST), Ikeda, Osaka 563-8577, Japan

Received: July 26, 2006; In Final Form: September 20, 2006

Reactions of gadolinium atoms and dimers with carbon monoxide molecules in solid argon have been studied using matrix isolation infrared absorption spectroscopy. Mononuclear $Gd(CO)_x$ ($x = 1-3$) and dinuclear $Gd_2(CO)_x$ ($x = 1, 2$) gadolinium carbonyls formed spontaneously on annealing. The $Gd(CO)_x$ complexes are CO terminal-bonded carbonyls, whereas the Gd_2CO and $Gd_2(CO)_2$ carbonyl complexes were characterized to have asymmetrically bridging and side-on-bonded CO, which are drastically activated with remarkably low C−O stretching frequencies. The cyclic $Gd_2(\mu\text{-C})(\mu\text{-O})$ and $Gd_3(\mu\text{-C})(\mu\text{-O})$ molecules in which the C−O triple bond is completely cleaved were also formed on annealing. The $Gd_2(CO)_2$ complex rearranged to the more stable c-$Gd_2(\mu\text{-O})(\mu\text{-CCO})$ isomer, which also has a four-membered ring structure with one CO being completely activated.

Introduction

Carbon monoxide activation and reduction are very important in a great many industrial processes such as hydroformylation, alcohol synthesis, and acid synthesis.[1,2] Reactions of metal atoms and small clusters with carbon monoxide serve as ideal models for fundamental understanding of the multifaceted mechanisms of carbon monoxide activation by metal complexes and surfaces. Numerous experimental and theoretical investigations have been focused on the reactions of transition-metal and main group element atoms and small clusters with CO, and a variety of transition-metal and main group metal carbonyl complexes have been characterized.[3−11]

Coordination of CO to the metal centers weakens the π bonds of CO, which can activate CO toward further reaction. Previous investigations have demonstrated C−O bond activation through some early transition-metal and actinide metal carbonyl complexes.[12−15] The monocarbonyls of Nb, Th, and U can be isomerized to the inserted carbide-oxide molecules CMO, and the dicarbonyls of the Ti and V groups, and the actinide metals Th and U photochemically rearranged to the OMCCO and OTh-(η^3-CCO) or (η^2-C_2)UO_2 isomers. Recent studies showed that group IIIB metal dimers reacted with CO to form homoleptic dinuclear metal carbonyls with asymmetrically bridging and side-on-bonded CO, which is drastically activated with remarkably low C−O stretching frequencies.[16,17] The complexes rearrange to the planar cyclic $M_2(\mu\text{-C})(\mu\text{-O})$ isomers with the C−O bond being completely cleaved.

The reactions of lanthanide metal atoms with carbon monoxide have also gained considerable attention. A series of binary lanthanide metal carbonyls were prepared and were spectroscopically characterized in solid noble gas matrixes.[18−20] The interaction between lanthanide metal atoms and CO has also been the subject of theoretical studies.[21] Recent investigations in our laboratory on the reactions of lanthanide metal atoms and dimers with CO have characterized the cerium carbonyls: end-on-bonded CeCO and side-on-bonded Ce_2CO.[22] The carbonyl complexes rearranged to the CCeO and c-$Ce_2(\mu\text{-C})(\mu\text{-O})$ molecules, where Ce and Ce_2 are inserted into the CO triple bond. Here, we report a combined matrix isolation infrared spectroscopic and theoretical study of the reactions of gadolinium atoms and small clusters with carbon monoxide. Gadolinium is a typical lanthanide metal with a half-filled 4f shell and one valence electron in 5d orbitals. We will show that besides the mononuclear gadolinium carbonyls, the dinuclear carbonyls with asymmetrically bridging and side-on-bonded CO are also formed, and they rearranged to the cyclic $Gd_2(\mu\text{-C})(\mu\text{-O})$ and $Gd_2(\mu\text{-O})(\mu\text{-CCO})$ molecules, in which the C−O triple bond is completely cleaved.

Experimental and Theoretical Methods

The experimental setup for pulsed laser ablation and matrix isolation infrared absorption spectroscopic investigation has been described in detail previously.[23] Briefly, a Nd:YAG laser fundamental (1064 nm, 10 Hz repetition rate with 10-ns pulse width) was focused onto the rotating gadolinium metal target. The laser-ablated gadolinium atoms were co-deposited with CO in excess argon onto a CsI window cooled normally to 6 K by means of a closed-cycle helium refrigerator (ARS, 202N). Carbon monoxide (Shanghai BOC, 99.99%), $^{13}C^{16}O$ (99%, Cambridge Isotopic Laboratory), and $^{12}C^{18}O$ (95%, Isotec) were used to prepare the CO/Ar mixtures. In general, matrix samples were deposited for 1−2 h with a gas deposition rate of approximately 4 mmol per hour. After sample deposition, IR spectra were recorded on a Bruker IFS66V spectrometer at 0.5 cm^{-1} resolution using a liquid-nitrogen-cooled HgCdTe (MCT) detector for the spectral range of 4000−400 cm^{-1}. Samples were annealed at different temperatures and were subjected to broadband irradiation using a tungsten lamp or a high-pressure mercury arc lamp with glass filters.

* Authors to whom correspondence should be addressed. E-mail: mfzhou@fudan.edu.cn (Zhou), q.xu@aist.go.jp (Xu).
† Fudan University.
‡ National Institute of Advanced Industrial Science and Technology.

10.1021/jp064751k CCC: $33.50 © 2006 American Chemical Society
Published on Web 10/28/2006

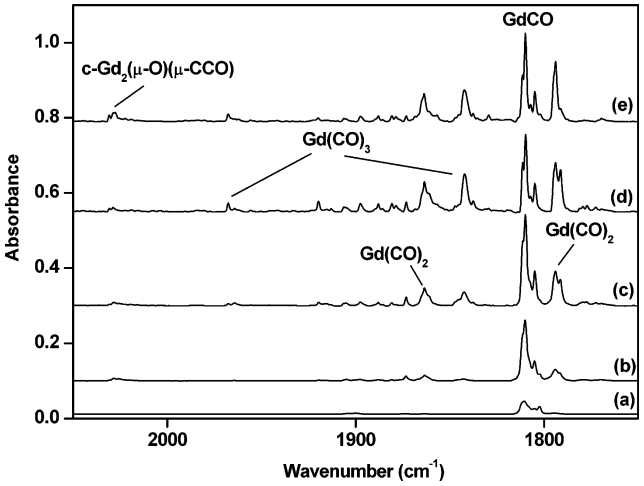

Figure 1. Infrared spectra in the 2050−1750 cm^{-1} region from co-deposition of laser-evaporated Gd atoms with 0.05% CO in argon. (a) One hour of sample deposition at 6 K, (b) after annealing to 25 K, (c) after annealing to 30 K, (d) after annealing to 35 K, and (e) after 20 min $\lambda > 500$ nm irradiation.

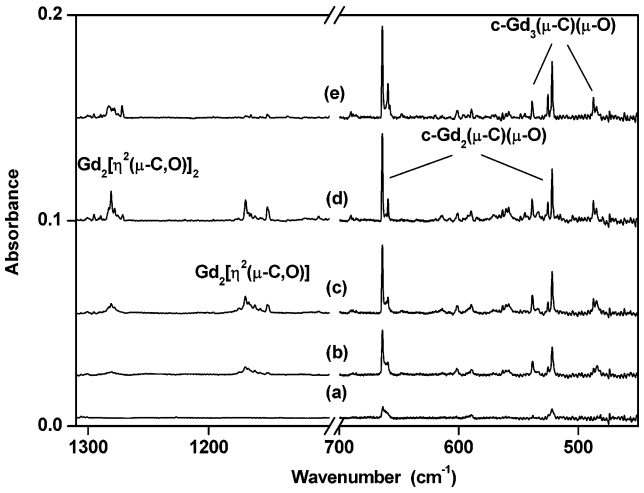

Figure 2. Infrared spectra in the 1310−1100 and 700−450 cm^{-1} regions from co-deposition of laser-evaporated Gd atoms with 0.05% CO in argon. (a) One hour of sample deposition at 6 K, (b) after annealing to 25 K, (c) after annealing to 30 K, (d) after annealing to 35 K, and (e) after 20 min $\lambda > 500$ nm irradiation.

Quantum chemical calculations were performed to determine the molecular structures and to help the assignments of vibrational frequencies of the observed reaction products. The PW91 functional and the TZ2P Slater basis set with frozen-core approximation to Gd 4d and C and O 1s were used.[24] Scalar relativistic effects were included via the zero-order regular approximation.[25] The vibrational frequencies and intensities were calculated by numerical differentiation.[26] Transition states were verified via intrinsic-reaction-coordinate calculations. All the calculations were performed using the ADF 2005.01 program.[27]

Results and Discussions

Infrared Spectra. A series of experiments were performed using different CO concentrations (ranging from 0.025% to 0.2% in argon) and different laser energies to control the relative concentrations of Gd and CO. The infrared spectra in selected regions with 0.05% CO in argon using relatively high laser energy are illustrated in Figures 1 and 2, respectively, with the product absorptions listed in Table 1. In the terminal C−O stretching frequency region (Figure 1), the absorption at 1809.7 cm^{-1} is weak on sample deposition, markedly increased on sample annealing to 25 and 30 K, but decreased on 35 K annealing. Absorptions at 1793.7, 1863.6, 1842.2, and 1967.6 cm^{-1} appeared on 25 K annealing and increased on 30 and 35 K annealing. These absorptions remained almost unchanged when the matrix was irradiated by the output of a tungsten lamp with a $\lambda > 500$ nm pass filter, during which a weak absorption at 2030.9 cm^{-1} was produced. In the 1100−1300 cm^{-1} frequency region (Figure 2), three weak absorptions at 1151.6, 1169.7, and 1281.0 cm^{-1} increased on sample annealing. The 1151.6 and 1169.7 cm^{-1} absorptions disappeared, while the 1281.0 cm^{-1} absorption markedly decreased under $\lambda > 500$ nm irradiation. In the low-frequency region, two pairs of absorptions at 664.0/521.9 cm^{-1} and 538.6/487.3 cm^{-1} were observed, which increased on annealing and upon $\lambda > 500$ nm irradiation.

Similar experiments were performed using isotopically labeled $^{13}C^{16}O$, $^{12}C^{18}O$, $^{12}C^{16}O + {}^{13}C^{16}O$, and $^{12}C^{16}O + {}^{12}C^{18}O$ mixtures. The isotopic frequencies are also listed in Table 1. The spectra in selected regions using different isotopic CO samples are shown in Figures 3−6, respectively.

$Gd(CO)_{1-3}$. The absorptions at 1793.7, 1809.7, 1842.2, 1863.6, and 1967.6 cm^{-1} lie in the region expected for the C−O stretching vibrations of terminal-bonded metal carbonyl species. As listed in Table 1, all absorptions exhibited $^{12}C/^{13}C$ and $^{16}O/^{18}O$ isotopic ratios that are characteristic of C−O stretching vibrations. The behavior in the experiments with different CO concentrations and laser energies suggests that these absorptions are most likely due to mononuclear gadolinium carbonyl molecules. The 1809.7 cm^{-1} absorption is the only product absorption observed in the terminal C−O stretching frequency region after sample deposition. In the mixed $^{12}C^{16}O + {}^{13}C^{16}O$ and $^{12}C^{16}O + {}^{12}C^{18}O$ experiments, only the pure isotopic counterparts were observed, which indicate that only one CO unit is involved in this vibration. Therefore, the 1809.7 cm^{-1} absorption is assigned to the GdCO molecule. The geometry

TABLE 1: Infrared Absorptions (cm^{-1}) from Co-Deposition of Laser-Ablated Gd Atoms and Clusters with CO in Solid Argon

^{12}CO	^{13}CO	$^{12}CO+{}^{13}CO$	$C^{18}O$	$C^{16}O+C^{18}O$	assignment
2030.9	1966.6	2030.9, 2021.1, 1976.7, 1966.6	2012.4	2030.9, 2012.4	c-Gd_2(μ-O)(μ-CCO) CCO str.
2027.6	1963.9	2027.6, 2018.2, 1973.6, 1963.9	2008.5	2027.6, 2008.5	c-Gd_2(μ-O)(μ-CCO) CCO str. site
1967.6	1923.3	1967.6, 1955.7, 1941.5, 1923.3	1922.4	1967.6, 1955.6, 1941.3, 1922.4	$Gd(CO)_3$ sym CO str.
1863.6	1821.7	1863.6, 1848.3, 1821.7	1820.8	1863.6, 1848.1, 1820.8	$Gd(CO)_2$ sym CO str.
1842.2	1802.1	1842.2, 1824.8, ..., 1802.1	1798.0	1842.2, 1822.9, ..., 1798.0	$Gd(CO)_3$ asym CO str.
1809.7	1769.5	1809.7, 1769.5	1767.9	1809.7, 1767.9	GdCO CO str.
1793.7	1753.9		1752.0		$Gd(CO)_2$ asym CO str.
1281.0	1251.4	1281.0, 1262.5, 1251.4	1253.6	1281.0, 1264.6, 1253.6	$Gd_2[\eta^2(\mu\text{-C,O})]_2$ asym CO str.
1169.7	1140.7	1169.7, 1140.7	1147.5	1169.7, 1147.5	$Gd_2[\eta^2(\mu\text{-C,O})]$ CO str.
1151.6	1123.3	1151.6, 1123.3	1130.7	1151.6, 1130.7	$Gd_2[\eta^2(\mu\text{-C,O})]$ site
664.0	644.1	664.0, 644.1	658.8	664.0, 658.8	c-Gd_2(μ-C)(μ-O)
521.9	517.1	521.9, 517.1	498.9	521.9, 498.9	c-Gd_2(μ-C)(μ-O)
538.6	531.8	538.6, 531.8	521.4		c-Gd_3(μ-C)(μ-O)
487.3	472.2	487.3, 472.2	480.2	487.3, 480.2	c-Gd_3(μ-C)(μ-O)

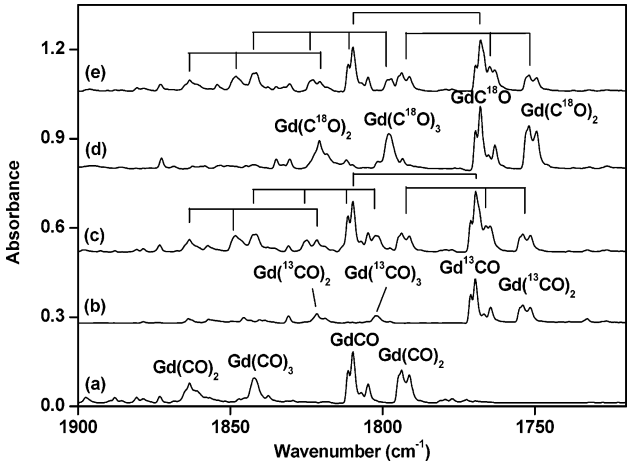

Figure 3. Infrared spectra in the 1900−1720 cm^{-1} region from co-deposition of laser-ablated Gd atoms and clusters with isotopic labeled CO in excess argon. Spectra were taken after 1 h of sample deposition followed by 35 K annealing. (a) 0.1% $^{12}C^{16}O$, (b) 0.1% $^{13}C^{16}O$, (c) 0.05% $^{12}C^{16}O$ + 0.05% $^{13}C^{16}O$, (d) 0.1% $^{12}C^{18}O$, and (e) 0.05% $^{12}C^{16}O$ + 0.05% $^{12}C^{18}O$.

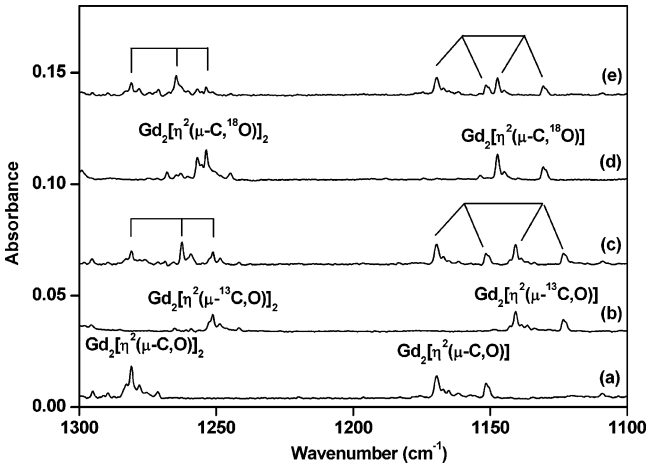

Figure 4. Infrared spectra in the 1300−1100 cm^{-1} region from co-deposition of laser-ablated Gd atoms and clusters with isotopic labeled CO in excess argon. Spectra were taken after 1 h of sample deposition followed by 35 K annealing. (a) 0.1% $^{12}C^{16}O$, (b) 0.1% $^{13}C^{16}O$, (c) 0.05% $^{12}C^{16}O$ + 0.05% $^{13}C^{16}O$, (d) 0.1% $^{12}C^{18}O$, and (e) 0.05% $^{12}C^{16}O$ + 0.05% $^{12}C^{18}O$.

and vibrational frequencies of GdCO were previously addressed by Hong et al. by using the density functional method with gradient correction and quasi-relativistic correction.[21] These calculations predicted that carbon monoxide preferentially coordinates to the metal atom with the C end to form the linear GdCO carbonyl. The ground state of GdCO has a spin multiplicity of 11. Our DFT/PW91 calculations are in good agreement with Hong et al's results. The C−O stretching frequency of ground-state GdCO was predicted to be 1817.4 cm^{-1}, see Table 2, very close to the experimental value.

The 1863.6 and 1793.7 cm^{-1} absorptions appeared together on annealing and are favored relative to the GdCO absorption in higher CO concentration experiments. In the mixed $^{12}C^{16}O$ + $^{13}C^{16}O$ experiment, the upper mode splits into a triplet at 1863.6, 1848.3, and 1821.7 cm^{-1}. A similar triplet at 1863.6, 1848.1, and 1820.8 cm^{-1} was observed in the mixed $^{12}C^{16}O$ + $^{12}C^{18}O$ experiment. The intermediate absorptions of the low mode in the mixed experiments were overlapped by the strong Gd^{13}CO and GdC^{18}O absorptions. These observations suggest that two equivalent CO subunits are involved in the molecule, and accordingly, we assign the 1863.6 and 1793.7 cm^{-1}

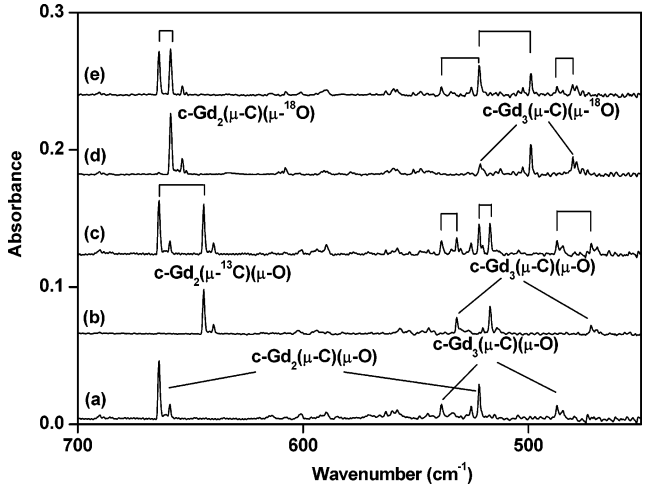

Figure 5. Infrared spectra in the 700−450 cm^{-1} region from co-deposition of laser-ablated Gd atoms and clusters with isotopic labeled CO in excess argon. Spectra were taken after 1 h of sample deposition followed by 35 K annealing. (a) 0.1% $^{12}C^{16}O$, (b) 0.1% $^{13}C^{16}O$, (c) 0.05% $^{12}C^{16}O$ + 0.05% $^{13}C^{16}O$, (d) 0.1% $^{12}C^{18}O$, and (e) 0.05% $^{12}C^{16}O$ + 0.05% $^{12}C^{18}O$.

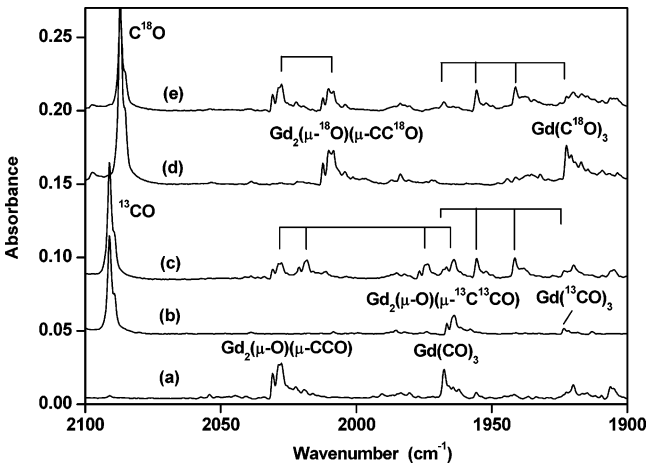

Figure 6. Infrared spectra in the 2100−1900 cm^{-1} region from co-deposition of laser-ablated Gd atoms and clusters with isotopic labeled CO in excess argon. Spectra were taken after 1 h of sample deposition followed by 30 K annealing and 15 min $\lambda > 500$ nm irradiation. (a) 0.1% $^{12}C^{16}O$, (b) 0.1% $^{13}C^{16}O$, (c) 0.05% $^{12}C^{16}O$ + 0.05% $^{13}C^{16}O$, (d) 0.1% $^{12}C^{18}O$, and (e) 0.05% $^{12}C^{16}O$ + 0.05% $^{12}C^{18}O$.

absorptions to the symmetric and antisymmetric C−O stretching modes of the bent Gd(CO)$_2$ molecule. DFT calculations predicted the Gd(CO)$_2$ molecule to have a $^{11}\Sigma_u$ ground state with a linear structure, and a bent $^{11}B_2$ state with a ∠CGdC = 67.6° is only 0.06 kcal/mol higher in energy. This is an extremely small energy diference that is within the errors of the method. Apparently, the predicted linear structure does not match the experimental observation, since the symmetric stretching mode of the linear molecule is IR inactive. The observation of two C−O stretching modes indicates that the molecule must be bent. The calculated antisymmetric and symmetric C−O stretching frequencies of the bent $^{11}B_2$ state also do not agree well with the experimental values. Recent studies indicate that some transition-metal as well as f element metal compounds trapped in solid matrixes are not "isolated" but are coordinated by multiple noble gas atoms.[28−32] In some cases, the coordination of noble gas atoms may induce ground-state reversal and large matrix frequency shifts. Our DFT calculations show that the $^{11}B_2$ state of Gd(CO)$_2$ can be coordinated by four argon atoms with a total Gd(CO)$_2$−Ar

TABLE 2: Calculated Vibrational Frequencies (Unscaled Harmonic Values in cm^{-1}) and Intensities (km/mol) of the Reaction Products[a]

	frequencies
GdCO ($^{11}\Sigma^-$)	1817.4 (965, σ)
$Gd(CO)_2$ ($^{11}\Sigma_u$)	1964.5 (0, σ_g), 1881.9 (3453, σ_u)
$Gd(CO)_2$ ($^{11}B_2$)	1943.0 (744, a_1), 1843.8 (1142, b_2)
$Gd(CO)_2Ar_4$ ($^{11}B_2$)	1862.1 (690, a_1), 1814.7 (1338, b_2)
$Gd(CO)_3$ ($^{11}A_2$)	1953.3 (461, a_1), 1874.5 (2759, e)
$Gd_2[\eta^2(\mu\text{-C,O})]$ ($^{15}A'$)	1207.5 (259, a′), 595.8 (3, a′), 452.5 (8, a′)
$Gd_2[\eta^2(\mu\text{-C,O})]_2$ ($^{15}A_g$)	1438.8 (0, a_g), 1347.8 (1081, b_u), 548.3(338, b_u), 468.1 (0, a_g)
c-$Gd_2(\mu\text{-C})(\mu\text{-O})$ ($^{15}B_2$)	649.3 (91, b_2), 589.2 (0, a_1), 496.7 (63, a_1)
c-$Gd_2(\mu\text{-O})(\mu\text{-CCO})$ ($^{15}B_2$)	2065.9 (1469, a_1), 1298.4 (3, a_1), 625.2 (10, b_2), 579.4 (6, b_1), 526.8 (53, a_1), 475.6 (47, b_2)
c-$Gd_3(\mu\text{-C})(\mu\text{-O})$ ($^{23}A'$)	611.6 (4, a′), 533.3 (14, a″), 533.2 (39, a′), 460.3 (71, a′) 402.0 (3, a″)

[a] Only the frequencies above 400 cm^{-1} are listed.

binding energy of 4.8 kcal/mol, whereas the linear $^{11}\Sigma_u$ state of $Gd(CO)_2$ does not form complex with argon. Therefore, the observed $Gd(CO)_2$ experimental vibrational frequencies suggest $Gd(CO)_2(Ar)_4$ is the carrier of the signal. The antisymmetric and symmetric C−O stretching frequencies of $Gd(CO)_2(Ar)_4$ were predicted at 1814.7 and 1862.1 cm^{-1} (Table 2), which are in good agreement with the experimental values. Similar calculations predict that the GdCO molecule does not coordinate Ar atoms.

The 1967.6 and 1842.2 cm^{-1} absorptions increased together on annealing. In the experiment with equimolar mixture of $^{12}C^{16}O$ and $^{13}C^{16}O$, a quartet was produced at 1967.6, 1955.7, 1941.5, and 1923.3 cm^{-1} with approximately 1:3:3:1 relative intensities. Similar mixed isotopic structure was observed in the mixed $^{12}C^{16}O + {}^{12}C^{18}O$ spectrum as shown in Figure 6. These spectral features indicate that the 1967.6 cm^{-1} absorption is due to a nondegenerate C−O stretching mode of a trigonal species with three equivalent CO subunits (statistically, a nondegenerate stretching vibrational mode which involves three equivalent CO subunits will split into four absorptions with approximately 1:3:3:1 relative intensities with a 1:1 mixture of $^{12}CO + {}^{13}CO$). The low mode most likely splits into a quartet with two weak intermediates (one intermediate is overlapped by the strong GdCO absorption) in the mixed experiments and is due to the doubly degenerate antisymmetric C−O stretching vibration (statistically, a doubly degenerate stretching vibrational mode which involves three equivalent CO subunits will split into four absorptions with approximately 5:3:3:5 relative intensities with a 1:1 mixture of $^{12}CO + {}^{13}CO$). The 1967.6 and 1842.2 cm^{-1} absorptions are assigned to the $Gd(CO)_3$ molecule with a C_{3v} symmetry. DFT calculations predicted that $Gd(CO)_3$ has a $^{11}A_2$ ground state with a C_{3v} structure (Figure 7). The doubly degenerate antisymmetric C−O stretching and the nondegenerate symmetric C−O stretching vibrations were computed at 1874.5 and 1953.3 cm^{-1}, respectively, with the calculated isotopic shifts and splittings in good agreement with the experimental values.

Binary gadolinium carbonyls ranging from GdCO to $Gd(CO)_6$ have been characterized in an earlier matrix isolation infrared study of reaction of thermal evaporated gadolinium atoms with carbon monoxide.[19] Absorptions at 1841, 1864, 1901, 1945, 1967, and 1986 cm^{-1} in solid argon were assigned to the $Gd(CO)_{1-6}$ molecules, respectively. It seems that the 1841 and 1967 cm^{-1} absorptions previously assigned to GdCO and $Gd(CO)_5$ correspond to the absorptions at 1842.2 and 1967.6 cm^{-1} that are assigned to $Gd(CO)_3$ in the present study. The 1809.7 and 1793.7 cm^{-1} absorptions due to low carbonyls were not observed in previous high CO concentration experiments (1% CO in Ar).[19]

Similar to transition-metal carbonyls, the bonding interactions in GdCO are dominated by the synergic donation of electrons in 5σ HOMO of CO to an empty σ orbital of the metal and the back-donation of the metal π electrons to the CO π^* orbital. The GdCO molecule has a $^{11}\Sigma^-$ ground state with an electron configuration of $(f^7)\ (1\sigma)^2\ (2\sigma)^1(1\pi)^2$, which correlates to the $f^7d^2s^1$ excited state of the Gd atom. The promotion of one s electron to a d orbital reduces the Gd−CO σ repulsion and increases the σ donation and π back-donation. The 4f orbital of Gd is corelike and does not participate in bonding. The 2σ molecular orbital is a quasi-atomic nonbonding orbital, which is largely Gd 6s in character. The doubly occupied 1σ MO is a bonding orbital that involves donation from the filled CO 5σ orbital onto the empty Gd 5dσ orbital; the doubly degenerate 1π MOs comprise extensive Gd 5dπ to CO 2π^* back-donation. Both the donation and back-donation interactions account for the chemical binding of CO to Gd. The bonding interactions in $Gd(CO)_2$ and $Gd(CO)_3$ are similar to those for the monocarbonyl. However, since there are two and three CO molecules to share the cost of s to d promotion, the s to d promotion is enhanced in $Gd(CO)_2$ and $Gd(CO)_3$.

$Gd_2[\eta^2(\mu\text{-C,O})]_{1-2}$. The absorptions at 1151.6, 1169.7, and 1281.0 cm^{-1} were only observed in the experiments with relatively high laser energy and low CO concentrations. The isotopic shifts indicate that all three absorptions are due to C−O stretching vibrations. The unusually low C−O stretching frequencies imply that the CO is sided-on bonded in these species. The 1169.7 and 1151.6 cm^{-1} absorptions exhibit quite similar isotopic frequency shifts. The mixed $^{12}C^{16}O + {}^{13}C^{16}O$ and $^{12}C^{16}O + {}^{12}C^{18}O$ spectra (Figure 4) clearly show that both the 1169.7 and 1151.6 cm^{-1} absorptions involve only one CO subunit. Therefore, we assign the 1169.7 and 1151.6 cm^{-1}

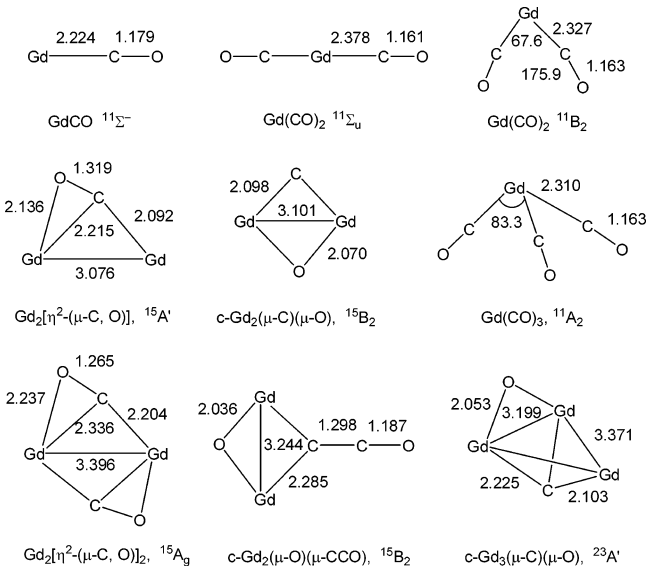

Figure 7. Optimized structures (bond lengths in angstrom, bond angles in degree) of the experimentally observed molecules.

absorptions to the CO side-on-bonded Gd_2CO molecule at two trapping sites. The 1281.0 cm^{-1} absorption splits into a triplet in the mixed $^{12}C^{16}O + {}^{13}C^{16}O$ and $^{12}C^{16}O + {}^{12}C^{18}O$ experiments and is assigned to the side-on-bonded $Gd_2(CO)_2$ molecule. The observation of only one C−O stretching mode suggests that the molecule is centrosymmetric.

DFT calculations were performed to support the assignment. The most stable structure of dinuclear monocarbonyl Gd_2CO was predicted to have a planar C_s structure with CO asymmetrically bridging and side-on bonded (Figure 7). The C atom is bonded to both Gd atoms with two inequivalent Gd−C bonds (2.092 and 2.215 Å). The C−O bond length is 1.319 Å, which is very close to those of the analogous $M_2[\eta^2(\mu\text{-C,O})]$ molecules recently reported (M = Sc, Y, La, and Ce).[16,17,22] The C−O stretching frequency was predicted to be 1207.5 cm^{-1}, which is 3.1% higher than the observed value. The $Gd_2[\eta^2(\mu\text{-C,O})]_2$ molecule was predicted to have a $^{15}A_g$ ground state with a planar C_{2h} symmetry as shown in Figure 7. Similar to $Gd_2[\eta^2(\mu\text{-C,O})]$, both CO's are asymmetrically bridging and side-on bonded to Gd_2. The C−O bond length was calculated to be 1.265 Å, shorter than that of $Gd_2[\eta^2(\mu\text{-C,O})]$. The antisymmetric C−O stretching vibration was computed at 1347.8 cm^{-1}, which is 5.0% higher than the experimental value.

The bonding interactions in the above-characterized side-on-coordinated dinuclear metal carbonyls are slightly different from those in end-on-coordinated mononuclear carbonyls. Taking $Gd_2[\eta^2(\mu\text{-C,O})]$ as an example, it was predicted to have a $^{15}A'$ ground state with an electron configuration of $(f^7)\ (f^7)\ (1a')^2\ (1a'')^2\ (2a')^2\ (3a')^2\ (4a')^2\ (2a'')^2$, which reflects the excited state of Gd_2 with the electronic configuration of $(f^7)\ (f^7)\ \sigma_g^2\pi_u$.[4] The 1a′ and 1a″ orbitals are largely CO 1π bonding orbitals and comprise CO to Gd donation. The 2a′ orbital is mainly CO 5σ in character and also involves CO to Gd donation. Hence, both the 5σ and 1π electrons of CO participate in donation. The 4a′ orbital is a Gd_2 σ bonding orbital and does not contribute to Gd_2−CO bonding. The 3a′ and 2a″ orbitals comprise significant Gd_2 bonding $\pi \rightarrow$ CO $2\pi^*$ back-donation. Both the donation from the filled 1π orbitals of CO and the back-donation from Gd_2 to CO 2π antibonding orbitals serve to weaken and therefore lengthen the CO bond. The weakening of the C−O bond leads to a large red-shift of the C−O stretching frequency of the $Gd_2[\eta^2(\mu\text{-C,O})]$ molecule. The Gd_2 molecule was previously determined to have a $^{19}\Sigma_g^-$ ground state with an electronic configuration of $(f^7)\ (f^7)\ \sigma_g^2\ \sigma_u^1\ \sigma_g^1\ \pi_u^2$.[33,34] The formation of $^{15}A'$ $Gd_2[\eta^2(\mu\text{-C,O})]$ from the ground-state Gd_2 ($^{19}\Sigma_g^-$) and CO involves two Gd_2 σ to π promotions. These promotions increase the Gd_2−CO bonding by decreasing the σ repulsion and increasing the Gd_2 $\pi \rightarrow$ CO $2\pi^*$ back-bonding. The binding energy of $Gd_2[\eta^2(\mu\text{-C,O})]$ with respect to $Gd_2(^{19}\Sigma_g^-)$ + CO was computed to be 67.3 kcal/mol, significantly larger than that of the end-on-bonded mononuclear carbonyls.

c-$Gd_x(\mu$-C)(μ-O) (x = 2, 3). Four absorptions were observed in the 700−500 cm^{-1} frequency region, which can be divided into two groups. Similar to the $Gd_2[\eta^2(\mu\text{-C,O})]$ absorptions, the intensities of these absorptions are stronger relative to the Gd-$(CO)_x$ absorptions in the experiments with higher laser energies and lower CO concentrations. The 664.0 and 521.9 cm^{-1} absorptions belong to the same molecule, and they are the dominate product absorptions on high-temperature annealing in the low-frequency region. The 664.0 cm^{-1} absorption showed a large shift (19.9 cm^{-1}) with $^{13}C^{16}O$ but a small shift (5.2 cm^{-1}) with $^{12}C^{18}O$. On the contrary, the 521.9 cm^{-1} absorption exhibited a small shift (4.8 cm^{-1}) with $^{13}C^{16}O$ but a large shift (23.0 cm^{-1}) with $^{12}C^{18}O$. The mixed $^{12}C^{16}O + {}^{13}C^{16}O$ and $^{12}C^{16}O + {}^{12}C^{18}O$ spectra (Figure 5, traces c and e) clearly show that only one O atom and one C atom are involved in the molecule. The band positions and isotopic frequency shifts suggest the involvement of a cyclic four-membered $Gd_2(\mu$-C)-(μ-O) structure. Accordingly, we assign the 664.0 and 521.9 cm^{-1} absorptions to the ring-puckering vibrations of the c-Gd_2-(μ-C)(μ-O) molecule.

The 538.6 and 487.3 cm^{-1} absorptions are due to different vibrational modes of the same molecule. The upper mode showed a small shift (6.8 cm^{-1}) with $^{13}C^{16}O$ but a large shift (17.2 cm^{-1}) with $^{12}C^{18}O$, while the low mode exhibited a small shift (7.1 cm^{-1}) with $^{12}C^{18}O$ but a large shift (15.1 cm^{-1}) with $^{13}C^{16}O$. The mixed $^{12}C^{16}O + {}^{13}C^{16}O$ and $^{12}C^{16}O + {}^{12}C^{18}O$ spectra (Figure 5, traces c and e) clearly demonstrate that only one C atom and one O atom are involved in each mode. These experimental observations imply that the molecule also involves a cyclic four-membered $Gd_2(\mu$-C)(μ-O) structural unit. The 538.6 and 487.3 cm^{-1} absorptions appeared after the c-$Gd_2(\mu$-C)(μ-O) absorptions. This observation suggests that the 538.6 and 487.3 cm^{-1} absorptions involve more Gd atoms than c-Gd_2-(μ-C)(μ-O), and therefore we assign these absorptions to the c-$Gd_3(\mu$-C)(μ-O) molecule. The frequency of more O involvement mode is slightly higher than that of c-$Gd_2(\mu$-C)(μ-O), but the frequency of more C involvement mode is much lower than that of c-$Gd_2(\mu$-C)(μ-O).

The c-$Gd_2(\mu$-C)(μ-O) molecule was predicted to have a $^{15}B_2$ ground state with a planar C_{2v} structure (Figure 7). The C−O separation in the ground state is computed to be 2.826 Å, indicating no direct bonding interaction between the C and O atoms. The experimentally observed modes were calculated at 649.3 and 496.7 cm^{-1}. The c-$Gd_3(\mu$-C)(μ-O) molecule was predicted to have a $^{23}A'$ ground state with a C_s symmetry (Figure 7). The c-$Gd_2(\mu$-C)(μ-O) subunit remains nearly planar. The third Gd atom lies in the molecular symmetry plane and interacts with the C and two Gd atoms with the Gd−C and Gd−Gd distances of 2.103 and 3.371 Å, respectively. The two ring-puckering vibrations were computed at 533.3 and 460.3 cm^{-1} with the isotopic frequency ratios in good agreement with the experimental values.

c-$Gd_2(\mu$-O)(μ-CCO). The 2030.9 cm^{-1} absorption lies in the region expected for a C−O stretching vibration. This band shifted to 1966.6 cm^{-1} with $^{13}C^{16}O$ and to 2012.4 cm^{-1} with $^{12}C^{18}O$, giving a $^{12}C/^{13}C$ isotopic frequency ratio of 1.0327 and a $^{16}O/^{18}O$ ratio of 1.0092. These ratios are significantly larger and smaller, respectively, than the diatomic CO ratios, suggesting that this C−O stretching mode is strongly coupled with another C atom. In the mixed $^{12}C^{16}O + {}^{13}C^{16}O$ experiment (Figure 6, trace c), a quartet at 2030.9, 2021.1, 1976.7, and 1966.6 cm^{-1} with approximately 1:1:1:1 relative intensities was observed, while in the mixed $^{12}C^{16}O + {}^{12}C^{18}O$ experiment (Figure 6, trace e), a doublet at 2030.9 and 2012.4 cm^{-1} was produced. These experimental observations indicate that the molecule involves a CCO subunit and is a reaction product from two CO molecules. This absorption was produced under $\lambda >$ 500 nm irradiation, during which only the side-on-bonded carbonyl absorptions were decreased, suggesting that it may be due to a structural isomer of $Gd_2[\eta^2(\mu\text{-C,O})]_2$. Geometry optimization on $Gd_2C_2O_2$ with a terminal CCO subunit found a stable structure shown in Figure 7. The molecule has a $^{15}B_2$ ground state with a planar C_{2v} symmetry. It involves a cyclic four-membered ring structure. The molecule was predicted to have a strong C−O stretching vibration at 2065.9 cm^{-1} with isotopic frequency ratios in excellent agreement with the experiment values. The other vibration modes were calculated

TABLE 3: Comparison of Calculated and Experimentally Observed Frequencies and Relative Intensities of the Product Molecules

molecule	mode	calcd	obsd	c/o ratio
c-$Gd_2(\mu$-O)(μ-CCO)	CCO str.	2065.9	2030.9	0.983
$Gd(CO)_3$	sym. CO str.	1953.3 (461)	1967.6 (0.18)	1.007
	asym. CO str.	1843.8 (1142)	1842.2 (1.00)	0.999
$Gd(CO)_2Ar_4$	sym. CO str.	1862.1 (690)	1863.6 (0.68)	1.001
	asym. CO str.	1814.7 (1338)	1793.7 (1.00)	0.988
GdCO	CO str.	1817.4 (965)	1809.7	0.996
$Gd_2[\eta^2(\mu$-C,O)$]_2$	asym. CO str.	1347.8 (1081)	1281.0	0.950
$Gd_2[\eta^2$ (μ-C,O)]	CO str.	1207.5 (259)	1169.7	0.969
c-$Gd_2(\mu$-C)(μ-O)	GdC str.	649.3 (91)	664.0 (1.00)	1.023
	GdO str.	496.7 (63)	521.9 (0.56)	1.051
c-$Gd_3(\mu$-C)(μ-O)	GdO str.	533.3 (53)	538.6 (0.65)	1.010
	GdC str.	460.3 (71)	487.3 (1.00)	1.059

to have much lower IR intensities and were not observed. In a previous study on the reactions of silicon atoms and small clusters with CO, a similar absorption at 2111.5 cm^{-1} has been assigned to the C−O stretching mode of an analogous c-Si_2-(μ-O)(μ-CCO) molecule, which was produced from the rearrangement of a $Si_2(CO)_2$ isomer.[11a]

Table 3 compares the calculated and experimentally observed band positions and relative IR intensities for the observed modes. Most of the calculated carbonyl stretching frequencies are slightly higher than the experimental values; the calculated modes of the cyclic molecules are slightly lower than the observed values. For the molecules that two modes were observed, the predicted relative IR intensities are also in reasonable agreement with the observed relative intensities.

Reaction Mechanism. Laser ablation of a gadolinium metal target produces gadolinium atoms and small clusters. The mononuclear $Gd(CO)_{1-3}$ and dinuclear $Gd_2[\eta^2(\mu$-C,O)$]_{1-2}$ gadolinium carbonyls were produced on annealing. These carbonyl species were formed by the reactions of gadolinium atoms and small clusters with CO in solid argon, eqs 1−5:

$$Gd(^9D) + CO(^1\Sigma_g^+) \rightarrow GdCO(^{11}\Sigma^-) \qquad \Delta E = -36.2 \text{ kcal/mol} \quad (1)$$

$$GdCO(^{11}\Sigma^-) + CO(^1\Sigma_g^+) \rightarrow Gd(CO)_2(^{11}B_2) \qquad \Delta E = -24.9 \text{ kcal/mol} \quad (2)$$

$$Gd(CO)_2(^{11}B_2) + CO(^1\Sigma_g^+) \rightarrow Gd(CO)_3(^{11}A_2) \qquad \Delta E = -34.6 \text{ kcal/mol} \quad (3)$$

$$Gd_2(^{19}\Sigma_g^-) + CO \rightarrow Gd_2[\eta^2(\mu\text{-C,O})](^{15}A') \qquad \Delta E = -67.3 \text{ kcal/mol} \quad (4)$$

$$Gd_2[\eta^2(\mu\text{-C,O})](^{15}A') + CO \rightarrow Gd_2[\eta^2(\mu\text{-C,O})]_2(^{15}A_g) \qquad \Delta E = -38.8 \text{ kcal/mol} \quad (5)$$

The c-$Gd_2(\mu$-C)(μ-O) and c-$Gd_3(\mu$-C)(μ-O) absorptions also increased on annealing. The c-$Gd_2(\mu$-C)(μ-O) molecules are formed from rearrangement of the $Gd_2[\eta^2(\mu$-C,O)] complex, eq 6. Theoretical calculations indicate that the cyclic $Gd_2(\mu$-C)(μ-O) molecule, in which the C−O triple bond is completely cleaved, is 25.4 kcal/mol more stable than the $Gd_2[\eta^2(\mu$-C,O)] complex. As shown in Figure 8, the C−O bond-breaking process proceeds via a bridge-bonded intermediate lying 8.8 kcal/mol higher in energy than the $Gd_2[\eta^2(\mu$-C,O)] complex. The energy barrier from the $Gd_2[\eta^2(\mu$-C,O)] complex to the CO activated c-$Gd_2(\mu$-C)(μ-O) isomer was estimated to be about 25.1 kcal/mol. Since the formation of $Gd_2[\eta^2(\mu$-C,O)] from Gd_2 + CO is exothermic by 67.3 kcal/mol, presumably this reaction exothermicity allows the products to surmount the energy barrier for C−O bond breaking, and the formation of c-$Gd_2(\mu$-C)(μ-O) is observed in solid argon. However, part of the initially formed $Gd_2[\eta^2(\mu$-C,O)] complex can also be stabilized as the matrix environment can effectively remove its internal thermal energy. The c-$Gd_3(\mu$-C)(μ-O) molecules are probably formed by addition eq 7, which is highly exothermic. The c-$Gd_2(\mu$-O)(μ-CCO) absorption increased only under visible light irradiation, during which the $Gd_2[\eta^2(\mu$-C,O)$]_2$ absorption decreased, which suggests that the c-$Gd_2(\mu$-O)(μ-CCO) molecules are formed by a photoinduced isomerization eq 8. Similar to eq 6, eq 8 proceeds via a bridge-bonded intermediate lying 15.3 kcal/mol higher in energy than the $Gd_2[\eta^2(\mu$-C,O)$]_2$ complex. The isomerization eq 8 is exothermic by 66.8 kcal/mol with an energy barrier of 34.4 kcal/mol. As shown in Figure 9, the transition state lies only 4.4 kcal/mol below the ground-state reactants: $Gd_2[\eta^2(\mu$-C,O)] ($^{15}A'$) + CO, the c-$Gd_2(\mu$-O)(μ-CCO) molecules were

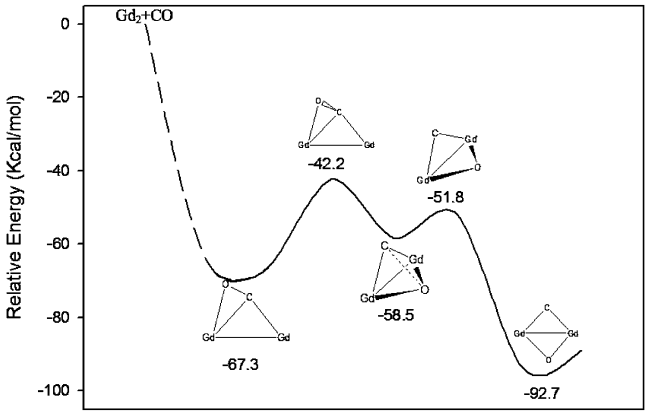

Figure 8. The reaction path and structures of the transition states and products in the Gd_2 + CO reaction. The dashed line indicates the computationally unexplored spin-crossing area.

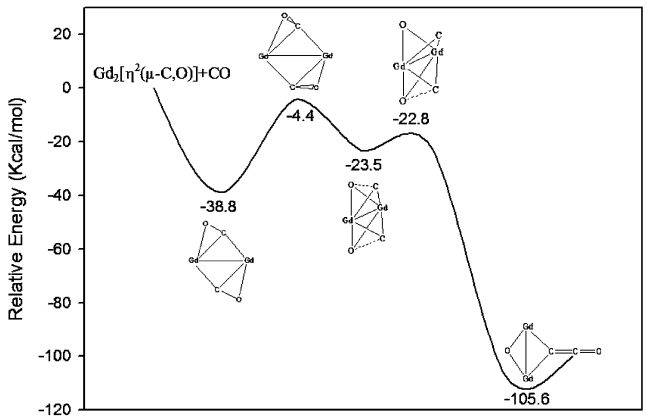

Figure 9. The reaction path and structures of the transition states and products in the Gd_2CO + CO reaction.

produced only under visible light irradiation, during which some excited electronic states may be involved.

$$Gd_2[\eta^2(\mu\text{-C,O})](^{15}A') \rightarrow c\text{-}Gd_2(\mu\text{-C})(\mu\text{-O})(^{15}B_2) \quad \Delta E = -25.4 \text{ kcal/mol} \quad (6)$$

$$c\text{-}Gd_2(\mu\text{-C})(\mu\text{-O})(^{15}B_2) + Gd(^9D) \rightarrow c\text{-}Gd_3(\mu\text{-C})(\mu\text{-O})(^{23}A') \quad \Delta E = -107.8 \text{ kcal/mol} \quad (7)$$

$$Gd_2[\eta^2(\mu\text{-C,O})]_2(^{15}A_g) \rightarrow c\text{-}Gd_2(\mu\text{-O})(\mu\text{-CCO})(^{15}B_2) \quad \Delta E = -66.8 \text{ kcal/mol} \quad (8)$$

Conclusions

Reactions of gadolinium atoms and dimers with carbon monoxide molecules in solid argon have been studied using matrix isolation infrared absorption spectroscopy. Mononuclear terminal-bonded gadolinium carbonyls $Gd(CO)_x$ ($x = 1-3$) were formed spontaneously on annealing. The GdCO monocarbonyl is predicted to have a $^{11}\Sigma$ ground state with a linear structure. The $Gd(CO)_2$ dicarbonyl is bent, while the $Gd(CO)_3$ molecule has a C_{3v} structure. Dinuclear gadolinium carbonyls $Gd_2(CO)_x$ ($x = 1, 2$) were also formed on annealing at low CO concentrations. The dinuclear carbonyls are characterized to have asymmetrically bridging and side-on-bonded CO(s), which are drastically activated with remarkably low C−O stretching frequencies. The cyclic $Gd_2(\mu\text{-C})(\mu\text{-O})$ and $Gd_3(\mu\text{-C})(\mu\text{-O})$ molecules in which the C−O triple bond is completely cleaved were also formed on annealing. The $Gd_2[\eta^2(\mu\text{-C,O})]_2$ complex rearranged to the more stable $c\text{-}Gd_2(\mu\text{-O})(\mu\text{-CCO})$ isomer, which also has a four-membered ring structure with one CO being completely activated.

Acknowledgment. This work is supported by NKBRSF (2004CB719501) and NNSFC (20433080).

References and Notes

(1) Muetterties, E. L.; Stein, J. *Chem. Rev.* **1979**, *79*, 479.
(2) Tumas, W.; Gitlin, B.; Rosan, A. M.; Yardley, J. T. *J. Am. Chem. Soc.* **1982**, *104*, 55.
(3) Willner, H.; Aubke, F. *Angew. Chem., Int. Ed. Engl.* **1997**, *36*, 2402.
(4) Lupinetti, A. J.; Strauss, S. H.; Frenking, G. *Prog. Inorg. Chem.* **2001**, *49*, 1.
(5) Zhou, M. F.; Andrews, L.; Bauschlicher, C. W., Jr. *Chem. Rev.* **2001**, *101*, 1931.
(6) Bridgeman, A. J. *Inorg. Chim. Acta*. **2001**, *321*, 27.
(7) Himmel, H. J.; Downs, A. J.; Greene, T. M. *Chem. Rev.* **2002**, *102*, 4191.
(8) (a) Tremblay, B.; Alikhani, M. E.; Manceron, L. *J. Phys. Chem. A* **2001**, *105*, 11388. (b) Tremblay, B.; Gutsev, G.; Manceron, L.; Andrews, L. *J. Phys. Chem. A* **2002**, *106*, 10525. (c) Tremblay, B.; Manceron, L.; Gutsev, G.; Andrews, L.; Partridge, H., III. *J. Chem. Phys.* **2002**, *117*, 8479.
(9) Jiang, L.; Xu, Q. *J. Phys. Chem. A* **2005**, *109*, 1026.
(10) (a) Zhou, M. F.; Tsumori, N.; Li, Z. H.; Fan, K. N.; Andrews, L.; Xu, Q. *J. Am. Chem. Soc.* **2002**, *124*, 12936. (b) Zhou, M. F.; Xu, Q.; Wang, Z. X.; Schleyer, P. R. *J. Am. Chem. Soc.* **2002**, *124*, 14854. (c) Zhou, M. F.; Wang, Z. X.; Schleyer, P. R.; Xu, Q. *ChemPhysChem*. **2003**, *4*, 763. (d) Zhou, M. F.; Jiang, L.; Xu, Q. *Chem.*—Eur. J. **2004**, *10*, 5817.
(11) (a) Zhou, M. F.; Jiang, L.; Xu, Q. *J. Chem. Phys.* **2004**, *121*, 10474. (b) Zhou, M. F.; Jiang, L.; Xu, Q. *J. Phys. Chem. A* **2005**, *109*, 3325. (c) Jiang, L.; Xu, Q. *J. Chem. Phys.* **2005**, *122*, 034505-1.
(12) Zhou, M.; Andrews, L.; Li, J.; Bursten, B. E. *J. Am. Chem. Soc.* **1999**, *121*, 9712.
(13) (a) Zhou, M.; Andrews, L.; Li, J.; Bursten, B. E. *J. Am. Chem. Soc.* **1999**, *121*, 12188. (b) Li, J.; Bursten, B. E.; Zhou, M. F.; Andrews, L. *Inorg. Chem.* **2001**, *40*, 5448.
(14) Zhou, M. F.; Andrews, L. *J. Phys. Chem. A* **1999**, *103*, 7785.
(15) Zhou, M. F.; Andrews, L. *J. Am. Chem. Soc.* **2000**, *122*, 1531.
(16) (a) Jiang, L.; Xu, Q. *J. Am. Chem. Soc.* **2005**, *127*, 42. (b) Jiang, L.; Xu, Q. *J. Phys. Chem. A* **2006**, *110*, 5636.
(17) Xu, Q.; Jiang, L.; Zou, R. *Chem.*—Eur. J. **2006**, *12*, 3226.
(18) Slater, J. L.; Devore, T. C.; Calder, V. *Inorg. Chem.* **1973**, *12*, 1918.
(19) (a) Slater, J. L.; DeVore, T. C.; Calder, V. *Inorg. Chem.* **1974**, *13*, 1808. (b) Sheline, R. K.; Slater, J. L. *Angew. Chem., Int. Ed. Engl.* **1975**, *14*, 309.
(20) Klotzbucher, W. E.; Petrukhina, M. A.; Sergeev, G. B. *Mendeleev Commun.* **1994**, *1*, 5.
(21) Hong, G. Y.; Lin, X. J.; Li, L. M.; Xu, G. X. *J. Phys. Chem. A* **1997**, *101*, 9314.
(22) Zhou, M. F.; Jin, X.; Li, J. *J. Phys. Chem. A* **2006**, *110*, 10206.
(23) (a) Chen, M. H.; Wang, X. F.; Zhang, L. N.; Yu, M.; Qin, Q. Z. *Chem. Phys.* **1999**, *242*, 81. (b) Zhou, M. F.; Zhang, L. N.; Dong, J.; Qin, Q. Z. *J. Am. Chem. Soc.* **2000**, *122*, 10680. (c) Wang, G. J.; Gong, Y.; Chen, M. H.; Zhou, M. F. *J. Am. Chem. Soc.* **2006**, *128*, 5974.
(24) (a) Perdew, J. P.; Wang, Y. *Phys. Rev. B* **1992**, *45*, 13244. (b) Perdew, J. P.; Chevary, J. A.; Vosko, S. H.; Jackson, K. A.; Pederson, M. R.; Singh, D. J.; Foilhais, C. *Phys. Rev. B* **1992**, *46*, 6671.
(25) van Lenthe, E.; Baerends, E. J.; Snijders, J. G. *J. Chem. Phys.* **1993**, *99*, 4597.
(26) Fan, L.; Ziegler, T. *J. Chem. Phys.* **1992**, *96*, 9005.
(27) (a) te Velde, G.; Bickelhaupt, F. M.; van Gisbergen, S. J. A.; Fonseca Guerra, C.; Baerends, E. J.; Snijders, J. G.; Ziegler, T. Chemistry with ADF. *J. Comput. Chem.* **2001**, *22*, 931. (b) Fonseca Guerra, C.; Snijders, J. G.; te Velde, G.; Baerends, E. J. *Theor. Chem. Acc.* **1998**, *99*, 391. (c) *ADF2005.01, SCM, Theoretical Chemistry*; Vrije Universiteit: Amsterdam, The Netherlands; http://www.scm.com.
(28) Li, J.; Bursten, B. E.; Liang, B.; Andrews, L. *Science* **2002**, *295*, 2242
(29) (a) Andrews, L.; Liang, B. Y.; Li, J.; Bursten, B. E. *J. Am. Chem. Soc.* **2003**, *125*, 3126. (b) Andrews, L.; Liang, B. Y.; Li, J.; Bursten, B. E. *Angew. Chem., Int. Ed.* **2000**, *39*, 4565.
(30) (a) Li, J.; Bursten, B. E.; Andrews, L.; Marsden, C. J. *J. Am. Chem. Soc.* **2004**, *126*, 3424. (b) Wang, X. F.; Andrews, L.; Li, J.; Bursten, B. E. *Angew. Chem., Int. Ed.* **2004**, *43*, 2554.
(31) (a) Zhao, Y. Y.; Wang, G. J.; Chen, M. H.; Zhou, M. F. *J. Phys. Chem. A* **2005**, *109*, 6621. (b) Zhao, Y. Y.; Gong, Y.; Chen, M. H.; Ding, C. F.; Zhou, M. F. *J. Phys. Chem. A* **2005**, *109*, 11765.
(32) Zhao, Y. Y.; Gong, Y.; Chen, M. H.; Ding, C. F.; Zhou, M. F. *J. Phys. Chem. A* **2006**, *110*, 1845.
(33) (a) Dolg, M.; Stoll, H.; Preuss, H. *THEOCHEM* **1992**, *227*, 239. (b) Cao, X.; Dolg, M. *Mol. Phys.* **2003**, *101*, 1967.
(34) Van Zee, R. J.; Li, S.; Weltner, W. *J. Chem. Phys.* **1994**, *100*, 4010.